

# Studies on the Mechanisms of Autophagy: Maturation of the Autophagic Vacuole

W. A. Dunn, Jr.

Department of Anatomy and Cell Biology, University of Florida College of Medicine, Gainesville, Florida 32610

**Abstract.** Data presented in the accompanying paper suggests nascent autophagic vacuoles are formed from RER (Dunn, W. A. 1990. *J. Cell Biol.* 110:1923–1933). In the present report, the maturation of newly formed or nascent autophagic vacuoles into degradative vacuoles was examined using morphological and biochemical methods combined with immunological probes. Within 15 min of formation, autophagic vacuoles acquired acid hydrolases and lysosomal membrane proteins, thus becoming degradative vacuoles. A previously undescribed type of autophagic vacuole was also identified having characteristics of both nascent and degradative vacuoles, but was different from lysosomes. This intermediate compartment contained only small amounts of cathepsin L in comparison to lysosomes and was bound by a double membrane, typical of nascent vacuoles. However, unlike nascent vacuoles yet comparable to degradative vacuoles, these vacuoles

were acidic and contained the lysosomal membrane protein, Igpl20, at the outer limiting membrane. The results were consistent with the stepwise acquisition of lysosomal membrane proteins and hydrolases. The presence of mannose-6-phosphate receptor in autophagic vacuoles suggested a possible role of this receptor in the delivery of newly synthesized hydrolases from the Golgi apparatus. However, tunicamycin had no significant effect on the amount of mature acid hydrolases present in a preparation of autophagic vacuoles isolated from a metrizamide gradient. Combined, the results suggested nascent autophagic vacuoles mature into degradative vacuoles in a stepwise fashion: (a) acquisition of lysosomal membrane proteins by fusing with a vesicle deficient in hydrolytic enzymes (e.g., prelysosome); (b) vacuole acidification; and (c) acquisition of hydrolases by fusing with preexisting lysosomes or Golgi apparatus-derived vesicles.

**P**ROTEINS are degraded by nonlysosomal and lysosomal mechanisms (13, 26, 28, 29). The cytoplasmic pathway involves ubiquitin targeting of susceptible proteins followed by proteasome hydrolysis (13). The endoplasmic reticulum and sarcoplasmic reticulum have been implicated in the degradation of abnormal, poorly folded proteins that have not oligomerized into functional proteins (22, 33). Proteins are believed to enter lysosomes by one of the following routes: lysosome membrane invagination (microautophagy), prp73-mediated transport, and fusion of lysosomes with endocytic vesicles or autophagic vacuoles (7, 11, 15, 16, 18, 26, 28). Studies by others suggest that endosomes become lysosomes through a complex maturation process that includes transport of proteins into and out of these acidic vesicles during maturation into lysosomes (15, 16, 18, 25). However, because researchers have been limited to interpretations of morphological and cytochemical data, they have suggested that autophagosomes become autolysosomes by simply fusing with preexisting lysosomes (2, 28). In response to an as yet unknown signal, a double-membrane bound vacuole forms, resulting in the sequestration of cytosolic components

into a nascent autophagic vacuole or autophagosome (AVi).<sup>1</sup> This vacuole then acquires acid hydrolases becoming a degradative autophagic vacuole or autolysosome (AVd). Whether or not AVis gradually mature into AVds as seen for the maturation of endocytic vesicles into lysosomes or that AVis become AVds by fusing with preexisting lysosomes is not known.

With the availability of specific immunological probes, I have been able to examine in more detail than earlier studies (2, 28, 30, 34) the events of vacuole formation and subsequent transition to an AVd. In the accompanying paper, I presented evidence that AVis form from ribosome-free segments of the RER. In this report, I examined the acidification of autophagic vacuoles, the incorporation of lysosomal enzymes and membrane proteins into these vacuoles, and the involvement of the mannose-6-phosphate receptor in the

1. *Abbreviations used in this paper:* AVd, degradative autophagic vacuole or autolysosome; AVi, nascent autophagic vacuole or autophagosome; DAMP, *N*-[3-[(2,4-dinitrophenyl)-amino]propyl]-*N*-(3-aminopropyl) methylamine dihydrochloride; IGFII-R/MPR, insulin-like growth factor II mannose-6-phosphate receptor.

delivery of hydrolases to these vacuoles. The identification of an unique population of autophagic vacuoles with characteristics similar to but significantly different from both AVi and AVd suggests that the AVi matures into an AVd.

## Materials and Methods

### Materials

Sprague-Dawley rats were purchased from Charles River Breeding Laboratories Inc. (Wilmington, MA) or University of Florida Breeding Facility (Gainesville, FL). New Zealand white female rabbits were obtained from Bunnyville Farms, Littleton, PA. Protein A (Pharmacia Inc., Piscataway, NJ) was iodinated using the chloramine T method (11). Immunogold probes were purchased from Janssen Life Science Products (Piscataway, NJ); horseradish peroxidase-conjugated sheep anti-mouse Fab and horseradish peroxidase-conjugated sheep anti-rabbit Fab from Biosys S. A. (Compiègne, France); LRGold resin from Polysciences (Warrington, PA); and Freund's adjuvant from Difco Laboratories Inc. (Detroit, MI). All other reagents were purchased from Sigma Chemical Co. (St. Louis, MO), from Fisher Scientific (Springfield, NJ), or from Bio-Rad Laboratories (New York, NY).

### Subcellular Fractionation of Liver Homogenates

Rough microsomes were prepared from a postmitochondrial supernatant as previously described (19). A fraction of low density vesicles was recovered from the 1.08–1.12 g/cc portion of a continuous sucrose gradient separation of a microsomal pellet (11). This fraction contained Golgi enzymes and endosomes (11). A lysosome-enriched fraction was isolated from liver homogenates obtained from rats previously injected with Triton WR-1339 (85 mg/100 g body wt) (20). The light lysosomes were separated from contaminating organelles by flotation through a discontinuous sucrose density gradient. Autophagic vacuoles were isolated from a 10,000-g pellet (12,000 rpm for 15 min) on a discontinuous metrizamide gradient following procedures outlined by Marzella et al. (24).

### Preparation of Antibodies

Triton-filled lysosomes were prepared from 30 g of liver as described above. Following procedures that have been used to purify liver plasma membrane proteins, lysosomes were solubilized in Tris-buffered NP-40 and recycled through a column of mouse anti-Igpl20 Ig (LylC6d) coupled to Sephadex 4B (4, 21). After numerous washings, lysosomal membrane glycoprotein 120 kD (Igp120) was eluted from the column with 0.25% (wt/vol) NP-40, 0.1 M NaCl, 0.1 M glycine-HCl, pH 3.0. Approximately 20 µg of Igp120

was then emulsified in Freund's complete adjuvant and injected into both popliteal lymph nodes of a rabbit (23). Rabbits were boosted intradermally with 10 µg of antigen at 2 and 4 wk. β-Glucuronidase was purified from rat preputial glands as previously described (14). The purified enzyme ran as a single protein band (68–70 kD) on SDS-PAGE. β-Glucuronidase (100 µg) was emulsified in Freund's complete adjuvant and injected intradermally at numerous sites on the rabbit's back. The rabbits were then boosted 2 wk later using 50 µg of antigen and bled periodically for 30 wk. Antisera were screened on Western blots of lysosome fractions. Anti-β-glucuronidase antibodies were purified on a column of purified β-glucuronidase coupled to Sepharose 4B as described previously (11).

### Liver Perfusion

Livers were excised from rats previously fasted for 20–24 h and cyclically perfused with media selected to enhance or inhibit autophagy (8–10, 26, 35). Livers were routinely perfused with a medium enriched with amino acids (plus 14 nM insulin) to inhibit the formation of AVi and allow the maturation of existing autophagic vacuoles to residual bodies. The medium was then switched to one depleted of amino acids (plus 86 nM glucagon) to initiate autophagy. When vacuole acidification was examined, *N*-[3-(2,4-dinitrophenyl)-amino]propyl]-*N*-(3-aminopropyl)methylamine (DAMP) was added at a final concentration of 50 µM to the nutrient-depleted medium and the livers perfused in the absence or presence of 50 µM monensin for 25 min.

### Cytochemistry

**Immunoperoxidase.** Livers were fixed by perfusion at 25°C with 2% paraformaldehyde/0.075 M lysine/0.01 M sodium periodate/0.037 M sodium phosphate, pH 7.4. Small cubes (1 mm<sup>3</sup>) of tissue were then fixed an additional 4 h at room temperature and frozen in 2-methylbutane cooled by liquid nitrogen. Antigens were localized at the ultrastructural level by incubating cryosections (15-µm thick) of tissue with the appropriate antisera, Ig, or affinity-purified primary antibody followed by a horseradish peroxidase conjugate of sheep anti-rabbit (or anti-mouse) Fab according to Brown and Farquhar (5).

**Immunogold.** Livers were fixed by perfusion as described above or with 1% glutaraldehyde/2% paraformaldehyde/0.025% CaCl<sub>2</sub>/0.1 M sodium cacodylate, pH 7.4 to insure adequate retention of low molecular weight DAMP. Portions of the liver were diced into 1-mm<sup>3</sup> blocks, washed with 50 mM NH<sub>4</sub>Cl in PBS, dehydrated in ethanol, and embedded in LRGold resin (9). The blocks were polymerized at –20°C using an ultraviolet lamp. Ultrathin sections were cut using a diamond knife (Diatome-US Co., Fort Washington, PA) on an Ultracut E microtome (Cambridge Inst., Deerfield, IL) and placed on 400 mesh nickel grids (Ernest F. Fullum, Inc., Schenectady, NY). Immunogold double labeling was done by incubating the sections with rabbit anti-cathepsin L Ig or rabbit anti-Igp120 antiserum at

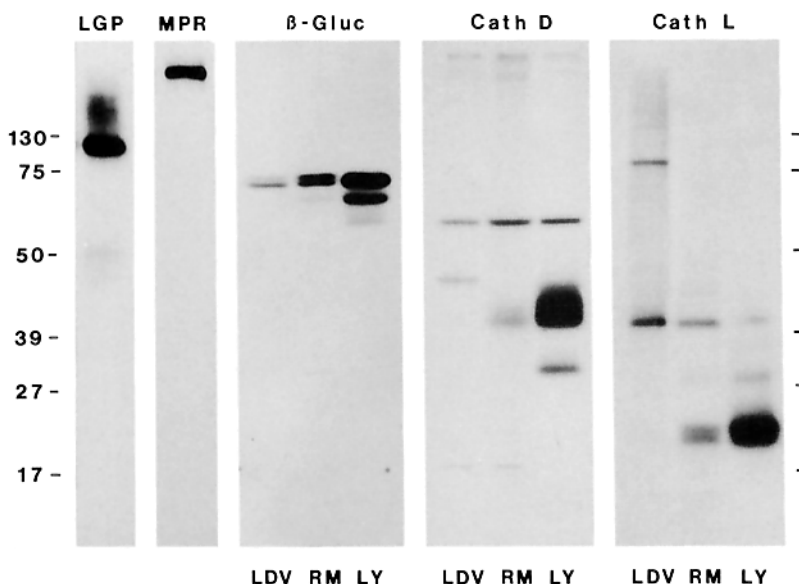


**Figure 1.** Characterization of antibodies on Western blots. Low density vesicles (LDV), rough microsomes (RM), and lysosomes (LY) were prepared as described in Materials and Methods, and their proteins (35 µg) separated by SDS-PAGE and transferred to nitrocellulose (10, 11). The immobilized proteins were then incubated with anti-Igp120 antiserum (LGP), and anti-IGFII receptor antiserum (MPR), affinity-purified anti-β-glucuronidase Ig (β-Gluc), anti-cathepsin L Ig (Cath L), anti-cathepsin D antiserum (Cath D), followed by <sup>125</sup>I-protein A (10, 11). Only 10 µg of purified lysosomes was applied to the gel for detecting cathepsin D and L.

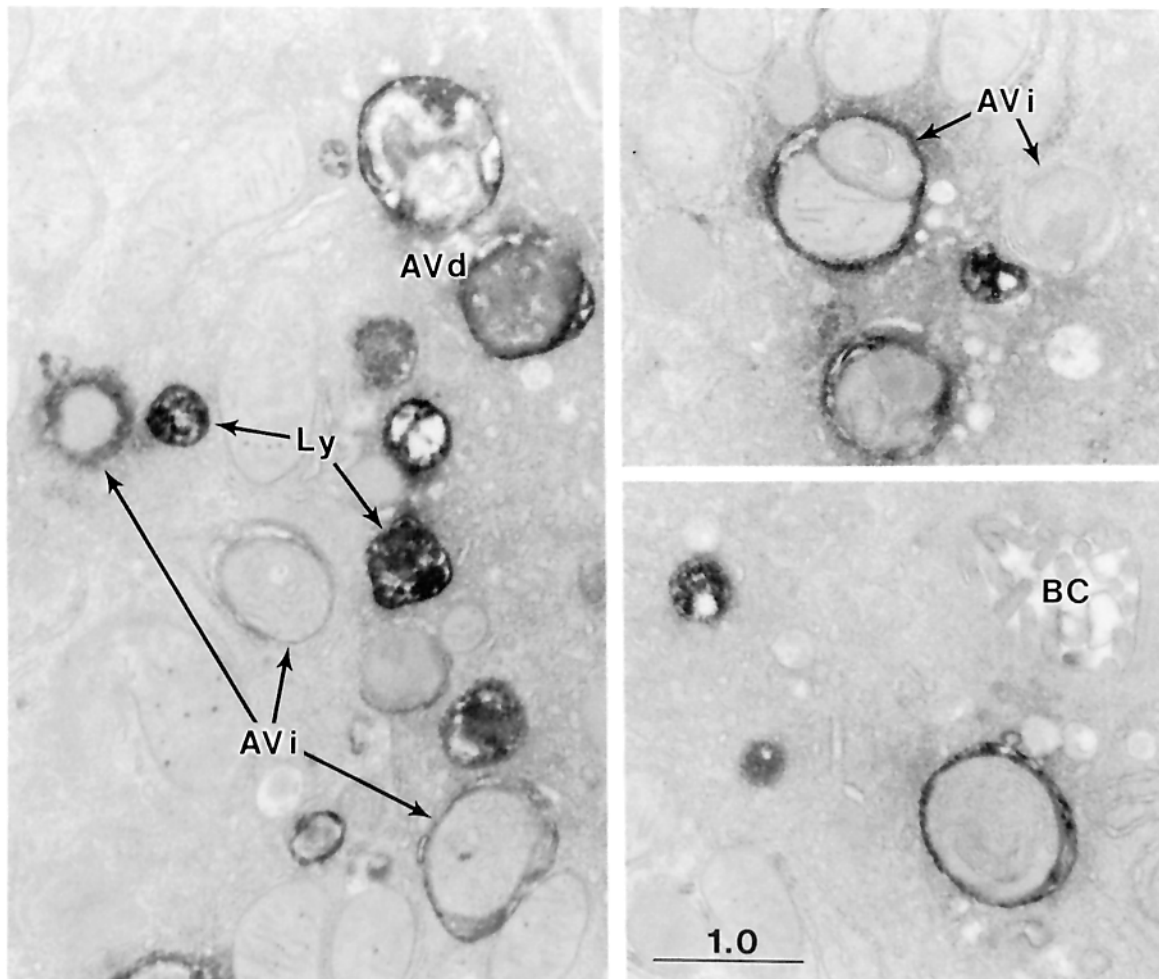


**Figure 2.** Immunolocalization of Igpl20 to autophagic vacuoles. Livers from rats previously fasted for 24 h were excised and perfused with an amino acid-enriched media containing insulin. At 90 min, the media was changed to one depleted of amino acids and containing glucagon and the liver perfused an additional 30 min. The livers were then fixed by perfusion and processed for immunoperoxidase cytochemistry. LGP120 was present in lysosomes (*Ly*), degradative autophagic vacuoles (*AVd*), and some nascent autophagic vacuoles (*AVi*). The reaction product was distributed throughout the lumen of lysosomes and degradative vacuoles but restricted to the region between the inner and outer membranes of nascent vacuoles. The results were consistent regardless of the antibody used (e.g., rabbit antiserum or mouse ascites obtained from Dr. I. Mellman [Yale University, New Haven, CT] or anti-Igpl20 antiserum described above). *BC*, bile canaliculus. Bar, 1.0  $\mu\text{m}$ .

22°C for 16 h followed by a 2-h incubation with a 10-nm gold conjugate of protein A. The sections were then sequentially incubated with mouse anti-DNP Ig for 2 h followed by goat anti-mouse conjugated to 5 nm gold for 1 h. The sections were washed extensively and stained with uranyl acetate and lead citrate before viewing (38).

## Results

### Characterization of Immunological Probes

Affinity-purified rat liver Igpl20 was used as an immunogen in rabbits and the resulting antisera recognized a heterogeneous protein of 110–130 kD on Western blots of purified lysosome fractions (Fig. 1). This blotting pattern was identical when using anti-Igpl20 antiserum characterized previously by Lewis et al. (data not shown) (21). Immunoperoxidase labeling of fixed liver tissue revealed that the antisera labeled predominately vesicles of various sizes presumed to be lysosomes (see Fig. 2).

Affinity-purified anti- $\beta$ -glucuronidase Ig recognized predominately two proteins with apparent molecular masses of 70 and 72 kD in low density vesicles (Golgi/endosome) and rough microsome fractions and a single band at 70 kD in lysosome fractions (Fig. 1). In addition, a second protein of 65 kD, presumed to be a proteolytic fragment, was observed in purified lysosome fractions. The presence of  $\beta$ -glucuronidase in Golgi vesicles and in portions of the RER was verified by immunoperoxidase staining of fixed liver tissue (data not shown).

Although the antibodies to cathepsin L, cathepsin D, and insulin-like growth factor type II/mannose-6-phosphate receptor (IGFII-R/MPR) have been characterized in some cells and tissues, the specificity of these probes has not been examined in rat liver tissue. Therefore, the antigens recognized by these antibodies were identified on Western blots of Golgi/endosome, rough microsomes, and lysosome fractions obtained from liver homogenates (Fig. 1). Anti-cathepsin L identified three major proteins (25, 41, and 80 kD) while

**Table I. Quantitation of Nascent Autophagic Vacuoles that Contain Lysosomal Proteins**

Antibody	Total AVi profiles counted	Percent of AVi labeled positive
<b>Membrane proteins</b>		
LGP120	184	49
LIMP I	58	33
LIMP V	45	38
<b>Luminal proteins</b>		
Acid phosphatase	231	4
$\beta$ -Glucuronidase	97	28
Cathepsin L	43	30
Cathepsin D	70	40

Livers were perfused with an amino acid-enriched medium containing insulin for 90 min and then switched to a medium depleted of amino acids containing glucagon for an additional 30 min. The livers were fixed and processed for immunoperoxidase cytochemistry (5). Blocks (two to three) of embedded tissue from duplicate experiments were cut and AVIs identified using morphologic criteria (see reference 11 and Figs. 2, 3, and 4). Those AVIs that contained label were quantified and tabulated as a percentage of the total number of AVIs counted.

anti-cathepsin D recognized three different proteins (31, 44, and 53 kD). Mature cathepsin L (25 kD) was found almost exclusively in the lysosome fraction. The 41-kD protein was found only in Golgi/endosome and rough microsome fractions and is comparable to the molecular mass reported for the precursor form of cathepsin L (27). In addition, the amount of this protein decreased to 20% of control when livers were perfused with cycloheximide (data not shown). Therefore, the evidence suggests that the 41-kD protein is the precursor form of this proteinase. A similar pattern of labeling was observed for precursor (53 kD) and mature (44 and 31 kD) forms of cathepsin D (12, 32). Anti-IGFII-R/MPR antibodies recognized only one protein migrating at the top of the gel as expected for this 270-kD receptor (17).

#### **Immunolocalization of Lysosomal Proteins to Autophagic Vacuoles**

In the accompanying paper, I reported that AVIs originated

from the RER (9). These vacuoles eventually become degradative vacuoles containing acid phosphatase, aryl sulfatase, and cathepsin D activities (2, 24). However, the presence of lysosome membrane proteins has not been established. I have used antibodies to lysosome membrane proteins and to lysosome hydrolases to visualize the presence and distribution of these proteins within the AVIs and AVds formed at 30 min of perfusion with nutrient-depleted medium.

**Membrane Proteins.** The lysosomal membrane antigen, lgp120, was localized to a substantial number of double-membrane bound autophagic vacuoles (Fig. 2 and Table I). The reaction product did not diffuse throughout the vacuolar lumen as seen with lysosomal labeling but was limited to the area between the inner and outer membrane. Labeling of AVds was clearly evident with reaction product diffusing throughout the vacuole. It should be noted that at this time the inner membrane is no longer intact. The appearance of the reaction precipitate within the vacuole was due to diffusion of the reaction product and not to the presence of soluble antigen. Immunogold localization of lgp120 was restricted to the limiting membrane of autophagic vacuoles (see Fig. 6).

The above results were further substantiated using monoclonal antibodies specific for two different lysosome integral membrane proteins, LIMP I (35–50 kD) and LIMP V (93 kD) (3, 36, 37). These proteins were localized to lysosomes including AVds and to a significant number of autophagic vacuoles limited by a double membrane (Fig. 3 and Table I). As seen with lgp120, the reaction product was restricted to the area between the inner and outer membranes.

**Matrix Proteins.** By using a cytochemical approach to examine enzyme activities, others have shown that acid phosphatase and aryl sulfatase activities are found in AVds but not AVIs (2). For this study, immunological probes were used to identify the presence of specific hydrolases within autophagic vacuoles. All hydrolases examined were present in AVds (Fig. 4). Cathepsin L, cathepsin D, and  $\beta$ -glucuronidase were also localized to a significant number of morphologically defined AVIs (Fig. 4 and Table I). However, acid phosphatase activity was absent from these early vacuoles

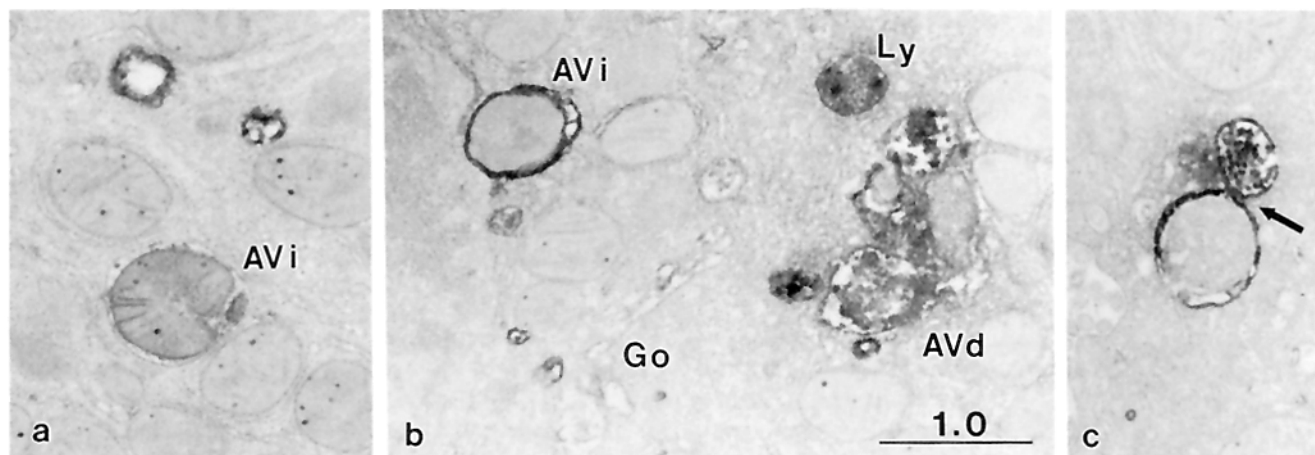


**Figure 3.** Immunolocalization of lysosomal integral membrane proteins (LIMP) to autophagic vacuoles. Livers were perfused under conditions described in Fig. 2 and processed for immunoperoxidase cytochemistry. Monoclonal antibodies to LIMP I (a) and LIMP V (b and c) labeled lysosomes (Ly), degradative autophagic vacuoles (AVd), and some nascent autophagic vacuoles (AVi). Acquisition of LIMPs by lysosome fusion was occasionally seen (arrow). Go, Golgi apparatus. Bar, 1.0  $\mu$ m.

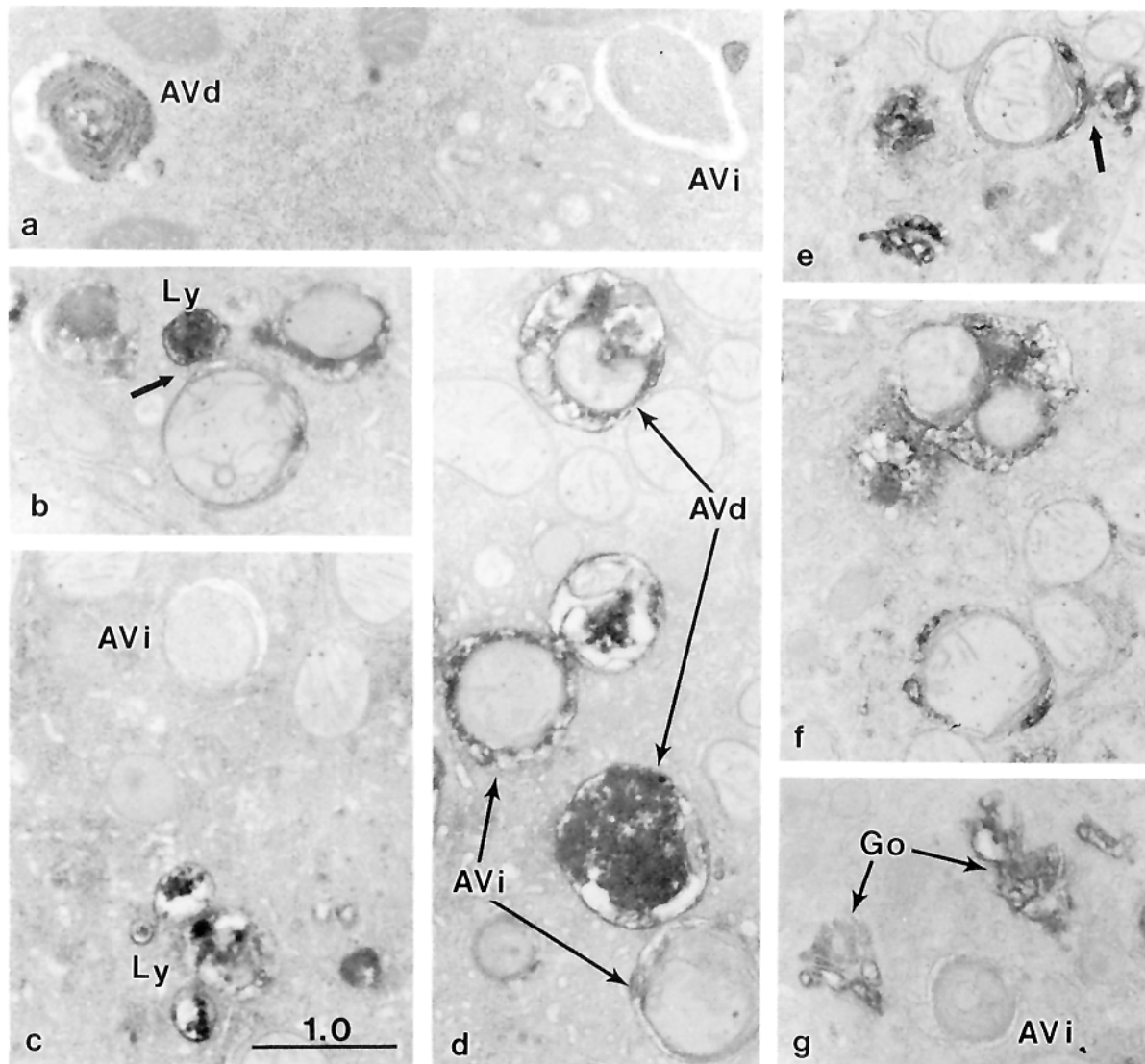


**Figure 4.** Immunolocalization of lysosomal hydrolases to autophagic vacuoles. Livers were perfused with nutrient-depleted media to initiate the autophagic response (see Fig. 2) and glutaraldehyde or formalin fixed by perfusion. (a) Cytochemical localization of acid phosphatase was done using cytidine 5'-monophosphate as a substrate (9).  $\beta$ -Glucuronidase (b and c), cathepsin L (d), and cathepsin D (e-g) were identified in fixed liver sections using immunoperoxidase methods (5). These hydrolases were found in lysosomes (Ly), degradative autophagic vacuoles (AVd), and occasionally in Golgi elements (Go), and rough endoplasmic reticulum (not shown). These proteins were also localized to the region between the inner and outer membranes of some nascent autophagic vacuoles (AVi). Nevertheless, a majority of the AVis did not contain hydrolases (a, c, and g). Profiles of lysosomes fusing with nascent autophagic vacuoles were also seen (arrows). Bar, 1.0  $\mu$ m.

(Table I). The distribution of the immunoperoxidase reaction product suggests that the hydrolases present were not accessible to the vacuolar contents but instead were confined to the space between the inner and outer membranes. Profiles of hydrolase-containing vesicles fusing with preexisting vacuoles (Fig. 4) were frequently observed, accounting for as much as 40% of the number of positively labeled AVis represented in Table I.

#### **Acidification of Autophagic Vacuoles**

I next examined the acidic nature of autophagic vacuoles using a probe for acidic compartments, DAMP (1). A majority of the DAMP was localized to vesicles and large vacuoles tentatively identified as lysosomes and AVd due to the pres-

ence of cathepsin L and Igpl20 (Figs. 5 and 6). The accumulation of DAMP into vacuoles containing cathepsin L was depressed by as much as 80% when the liver was exposed simultaneously to DAMP and monensin.

When comparing the levels of immunogold labeling for DAMP and cathepsin L, three populations of autophagic vacuoles were identified (Fig. 5 and Table II). Since antibody labeling varied with tissue fixation and antibody-incubation conditions, gold densities (gold particles/surface area) could not be related to precise amounts of antigen but rather to relative amounts present within the vacuoles. A population of AVis contained neither significant amounts of cathepsin L nor were they acidic, as determined by the absence of DAMP. Lysosomes and AVds comprised a second population

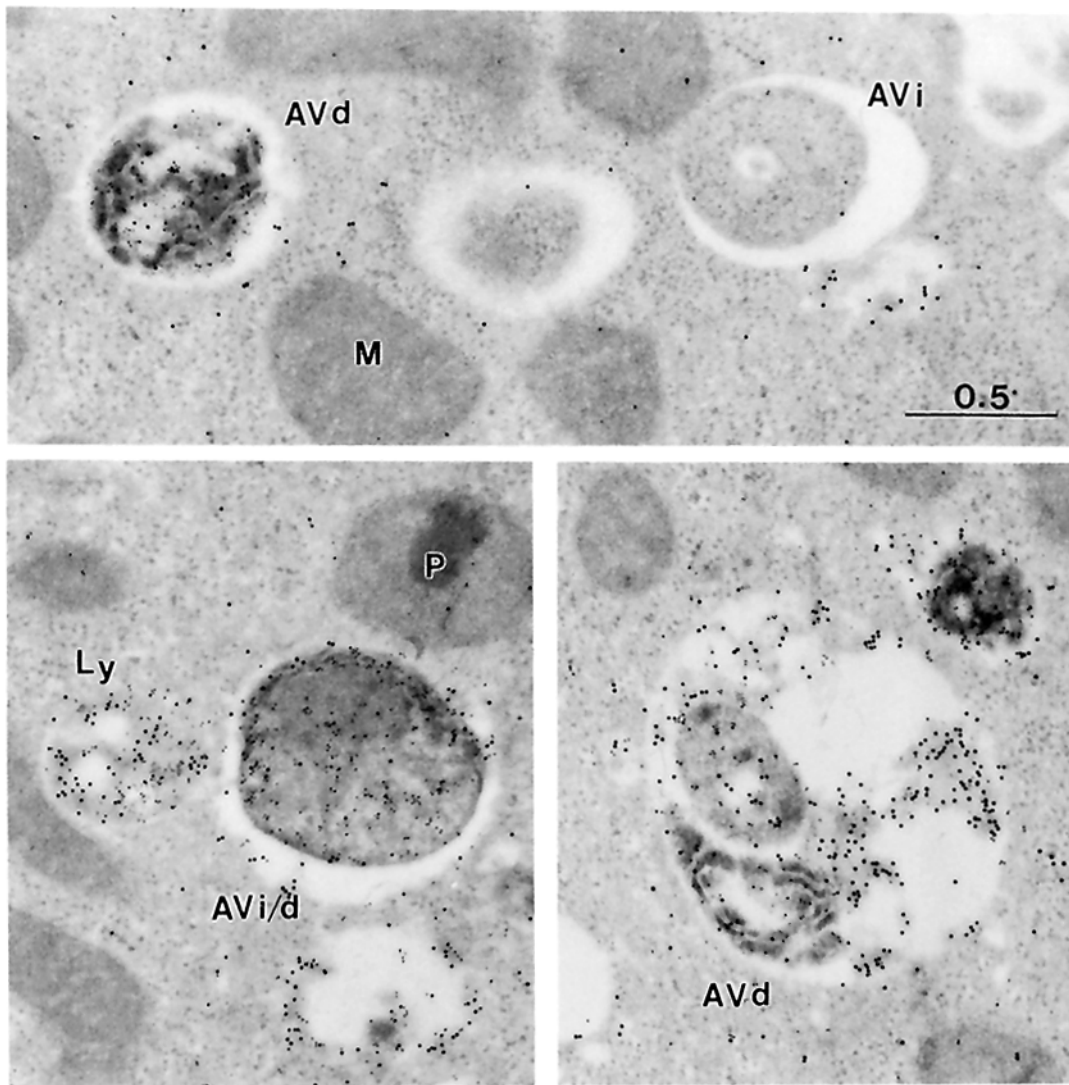


**Figure 5.** Acidification of autophagic vacuoles. Liver was excised and perfused for 90 min with media containing insulin and amino acids. The liver was then perfused an additional 30 min with amino acid-depleted media containing glucagon and DAMP (50  $\mu$ M), glutaraldehyde fixed by perfusion, and embedded in LRGold. DAMP (5 nm) and cathepsin L (10 nm) were colocalized using double labeling techniques described in Materials and Methods. Peroxisomes (*P*), mitochondria (*M*), and nuclei were not labeled by the immunological procedures. DAMP accumulated in lysosomes (*Ly*), degradative autophagic vacuoles (*AVd*), and some autophagic vacuoles (*AVi/d*) presumed to be predegradative due to the presence of a limiting double membrane and absence of cathepsin L. Cathepsin L was localized predominately to lysosomes and degradative autophagic vacuoles. Neither DAMP nor cathepsin L were identified in nascent autophagic vacuoles (*AVi*). Bar, 0.5  $\mu$ m.

of acidic vesicles that contained cathepsin L. Finally, a third population of autophagic vacuoles accumulated DAMP to the same extent as seen for lysosomes but contained very low levels of cathepsin L as estimated by the weak immunogold labeling. The relative amount of DAMP was significantly more than that observed for degradative vacuoles. In addition, Igpl20 was localized to the outer membrane of this acidic vacuole (Fig. 6). This vacuole (*AVi/d*) had characteristics of both an *AVi* (e.g., bound by a double membrane) and an *AVd* (e.g., acidic and contained Igpl20) and, therefore, was believed to be an intermediate in this pathway.

#### ***Mannose-6-PO<sub>4</sub> Receptor Is Localized to Nascent Autophagic Vacuoles***

IGFII-R/MPR has been implicated in the delivery of newly

synthesized acid hydrolases to prelysosomal vesicles identified as endosomes (5, 6, 18). I have localized in rat liver IGFII-R/MPR to Golgi cisternae, to vesicles presumed to be endosomes, and to 31% of the 111 *AVis* counted (Fig. 7). The absence of antigen from a majority of the vacuoles supported my concept that *AVis* were not formed from Golgi elements (9). However, the presence of the IGFII-R/MPR suggested a possible role for this receptor in the delivery of hydrolases to autophagic vacuoles. To further evaluate the role of this receptor in the transport of lysosomal enzymes to autophagic vacuoles, I compared the amounts of three specific lysosomal enzymes recovered from a preparation of autophagic vacuoles isolated from untreated and tunicamycin-treated livers. This fraction contained a heterogeneous population of predominately *AVds* (Fig. 8), but accounted for only 9–12%



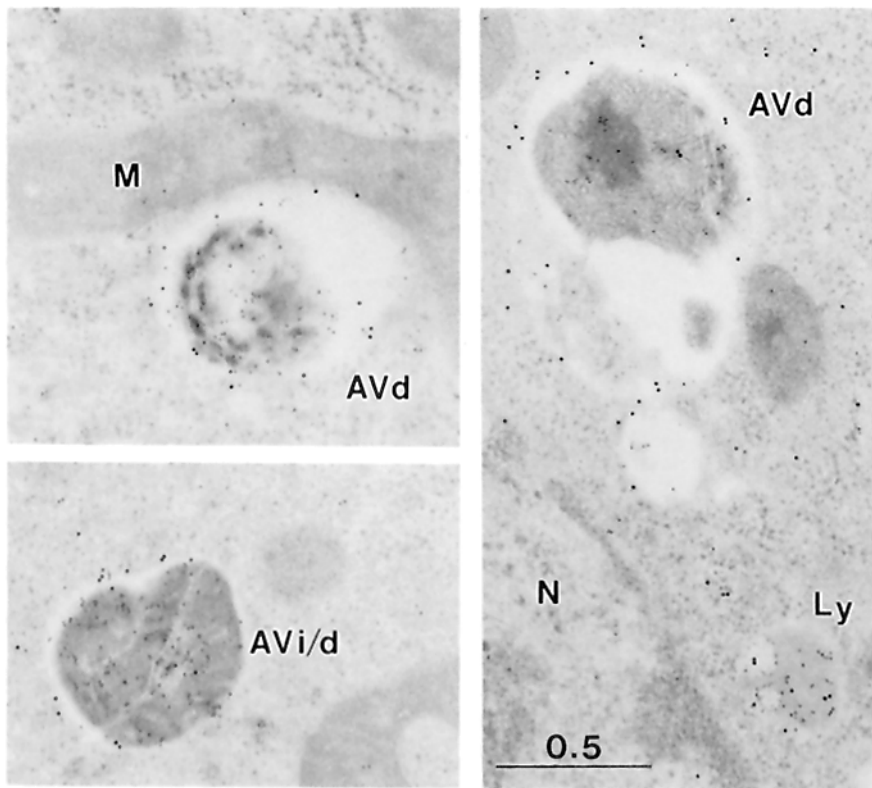


**Figure 6.** Localization of Igpl20 to acidic autophagic vacuoles. Liver was perfused under the conditions described in Fig. 6, fixed, and embedded in LRGold. DAMP (5 nm) and Igpl20 (10 nm) were colocalized using double labeling techniques as detailed in Materials and Methods. Immunogold labeling of peroxisomes, mitochondria (*M*), and nuclei (*N*) was not evident. LGPI20 was localized to the limiting membranes of acidic vesicles: lysosomes (*Ly*) and degradative autophagic vacuoles (*AVd*). In addition, Igpl20 was identified at the outer membrane of acidic predegradative autophagic vacuoles (*AVi/d*). Bar, 0.5  $\mu$ m.

of the total  $\beta$ -hexosaminidase and cathepsin L recovered from the gradient. Alkaline phosphodiesterase (plasma membrane) and sialyltransferase (Golgi membrane) were detected, but it was not clear whether some or all of these proteins were contained within autophagic vacuoles. Livers were perfused for 4 h with nutrient-depleted media containing tunicamycin, an inhibitor of N-linked glycosylation resulting in synthesis of nonglycosylated hydrolases that are unable to bind IGFII-R/MPR (12, 18, 32). This drug had no effect on the autophagic response as determined by measuring the percentage of cell volume represented by autophagic vacuoles (data not shown). In a tunicamycin-treated liver, IGFII-R/

MPR was localized predominately to Golgi cisternae and absent from 90% of the 74 AVis counted (data not shown). The amounts of mature lysosomal hydrolases ( $\beta$ -glucuronidase, cathepsin L, and cathepsin D) present in a preparation of autophagic vacuoles were not altered by this drug (Fig. 8). Furthermore, the glycosylated (41 kD) and unglycosylated (38 kD) precursors of cathepsin L were present in fractions obtained from untreated and treated livers, respectively.

### Discussion

Autophagy is a degradative pathway influenced by environ-

**Table II. Relative Concentrations of Cathepsin L and DAMP in Autophagic Vacuoles and Lysosomes as Determined by the Density of Immunogold Labeling**

	AVi (29)*	AVi/d (23)	AVd (23)	Lys (38)
	<i>gold particles/unit area</i>			
Cathepsin L	1.8 $\pm$ 0.3	7.1 $\pm$ 0.9 <sup>‡</sup>	21.5 $\pm$ 2.8 <sup>‡</sup>	37.0 $\pm$ 3.0
DAMP	1.3 $\pm$ 0.2	31.7 $\pm$ 4.4 <sup>§</sup>	14.3 $\pm$ 1.7 <sup>§</sup>	27.6 $\pm$ 3.0
Cathepsin L/DAMP		0.22	1.50	1.34

A liver was perfused with an amino acid-enriched medium containing insulin for 90 min and then switched to a medium depleted of amino acids containing glucagon and DAMP for an additional 30 min. The liver was fixed and embedded in LRGold. Sections on duplicate grids were sequentially labeled as described in Materials and Methods. Micrographs of vacuoles and lysosomes were printed at a final magnification of 50,000. Gold particles (5 nm, DAMP; and 10 nm, cathepsin L) were then counted and the data expressed relative to area measured on a digitizing tablet interfaced with Sigmascan software (Jandel Scientific, Corte Madera, CA). Lysosomes were identified as vesicles containing both cathepsin L and DAMP (Fig. 5). Vacuoles were categorized into groups (AVi, AVi/d, and AVd) based on morphology and the ratio of 10 nm/5 nm gold labeling (Fig. 5). Vacuoles bound by a double membrane and not labeled were AVis. Vacuoles bound by a double membrane with a labeling ratio of 10 nm/5 nm < 0.5 were identified as AVi/d. Vacuoles bound by a single membrane with a labeling ratio of 10 nm/5 nm > 1.0 were AVd. Background labeling over mitochondria was 1.1  $\pm$  0.1 5 nm particles/unit area and 1.2  $\pm$  0.1 10 nm particles/unit area. The measurements represent the mean  $\pm$  SEM. The labeling ratio of cathepsin L to DAMP was calculated from the mean values within the table.

\* The number in parentheses represents the total number of profiles counted.

<sup>‡</sup>  $P < 0.001$ .

<sup>§</sup>  $P < 0.001$ .

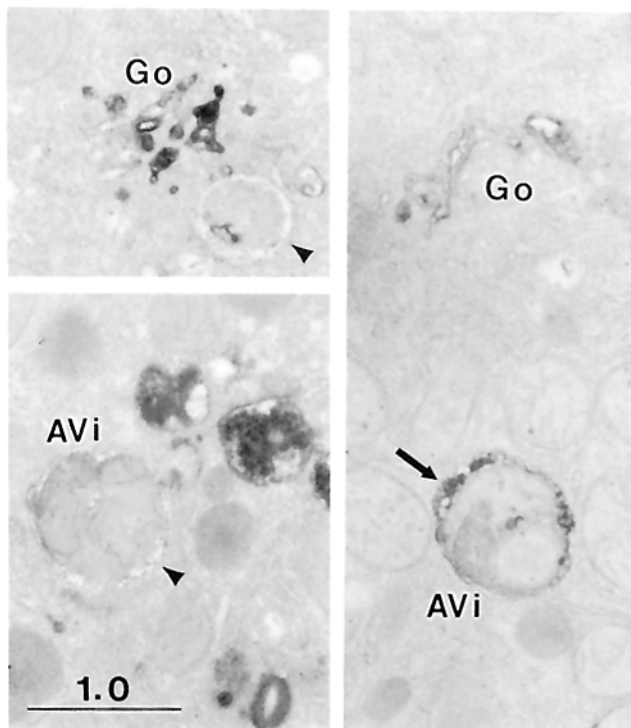


**Figure 7.** Immunolocalization of insulin-like growth factor II receptor (mannose-6-phosphate receptor) to autophagic vacuoles. IGFII-R/MPR was localized by immunoperoxidase methods on fixed tissue sections obtained from livers perfused under the conditions described in Fig. 2. The distribution of this receptor was restricted to a few Golgi cisternae (*Go*), vesicles presumed to be endosomes, and plasma membrane (not shown). Reaction product was also localized to the region between the two limiting membranes (*arrow*) of some nascent autophagic vacuoles (*AVi*). However, many vacuoles were not labeled (*arrowheads*). Bar, 1.0  $\mu\text{m}$ .

mental factors with the potential to assist in and possibly dictate cellular responses to environmental changes. This proteolytic response may be necessary to replenish depleted amino acid and glucose levels or to eliminate cellular proteins allowing cellular remodeling (15, 26). Despite the importance of autophagy in cellular metabolism, very little is known about the mechanisms governing autophagic degradation of proteins. In the accompanying paper, I presented evidence that AVIs are formed from ribosome-depleted regions of the rough endoplasmic reticulum. Here, I examined the events involved in the maturation of the newly formed vacuole to become a degradative vacuole.

My results indicate that the incorporation of Igpl20 is coincident with vacuole acidification but apparently not with the acquisition of hydrolases. The ability to label the limiting membrane of double-membrane bound autophagic vacuoles by *Limax flavus* lectin suggests that Igpl20 found in these vacuoles is not an immature form delivered from the RER but rather a mature sialylated protein (Fig. 9). The most likely source of Igpl20 is a previously uncharacterized acidic vesicle that does not contain acid hydrolases, i.e., prelysosome.

Delivery of the acid hydrolases may occur by three possible mechanisms: (a) newly synthesized precursors arising

from the RER; (b) IGFII-R/MPR targeting of newly synthesized lysosomal hydrolases to these vacuoles; and (c) fusion with preexisting lysosomes. The possibility that IGFII-R/MPR delivers hydrolases to the autophagic vacuoles is supported by the identification of this receptor in AVIs (Fig. 7). Cathepsin L precursor is also found in a preparation of autophagic vacuoles, but whether this precursor is present within the vacuoles or contaminating Golgi elements is unknown. Many acid hydrolases are directed by this receptor from the Golgi elements into endosomes (18). Tunicamycin effectively inhibits receptor-mediated delivery of newly synthesized acid hydrolases to lysosomes resulting in a redistribution of IGFII-R/MPR from vesicles presumed to be endosomes or lysosomes to Golgi cisternae (6, 18, 32). The number of AVIs containing this receptor was decreased in the presence of this drug. However, the amount of lysosomal hydrolases recovered with isolated autophagic vacuoles was not significantly impaired suggesting that IGFII-R/MPR-mediated transport is not the only avenue for delivery of acid hydrolases. The nonglycosylated form of the cathepsin L precursor is found in a preparation of autophagic vacuoles isolated from a tunicamycin-treated liver. This form of cathepsin L lacks mannose-6-phosphate recognition and can be isolated on sucrose gradients with vesicles containing ribophorin II (i.e., RER), but not sialyltransferase (i.e., Golgi apparatus) (Fisher, D. L., and W. A. Dunn, unpublished data). Therefore, this precursor appears to be in autophagic vacuoles (not Golgi contaminants) and is presumed to arise from the RER that is either forming the vacuole or being sequestered by a vacuole. The data presented here do not directly address the acquisition of hydrolases from lysosomes. However, autophagic vacuoles have been shown to acquire iron particles from lysosomes previously loaded with thorotrast (6). Proteins from the endocytic pathway (e.g., EGF and its receptor) accumulate within AVds, but the route of entry either from an endosome or a lysosome has not been determined (9). Combined, the data suggest that autophagic vacuoles acquire acid hydrolases from three sources: Golgi/endosomes, RER, lysosomes.

The limiting membranes of newly formed AVIs are similar in protein composition to the RER (2, 9). However, upon careful morphological and biochemical characterization of autophagic vacuolar membranes, other workers have suggested that these membranes are unique (15, 28). The autophagic vacuole membrane contains high levels of unsaturated fatty acids as determined by osmium impregnation and binds cationized ferritin suggesting a negative charge (e.g., sialic acid) oriented toward the inside of the vacuole (30, 34). The results presented here suggest that autophagic vacuoles mature from one form to another resulting in a heterogeneous population of vacuoles with differing characteristics. I have characterized three types of autophagic vacuoles which are apparently interrelated (Fig. 10). The membranes of the AVIs and AVds are comparable to the RER and lysosomes, respectively. However, the membranes of the AVi/d are unique in that membrane proteins originating from RER and lysosomes are present. In addition, the inner and outer membranes differ in their protein content in that only proteins of the RER are found at the inner membrane. These membranes also differ morphologically as examined by freeze-fracture techniques (31). A detailed biochemical charac-



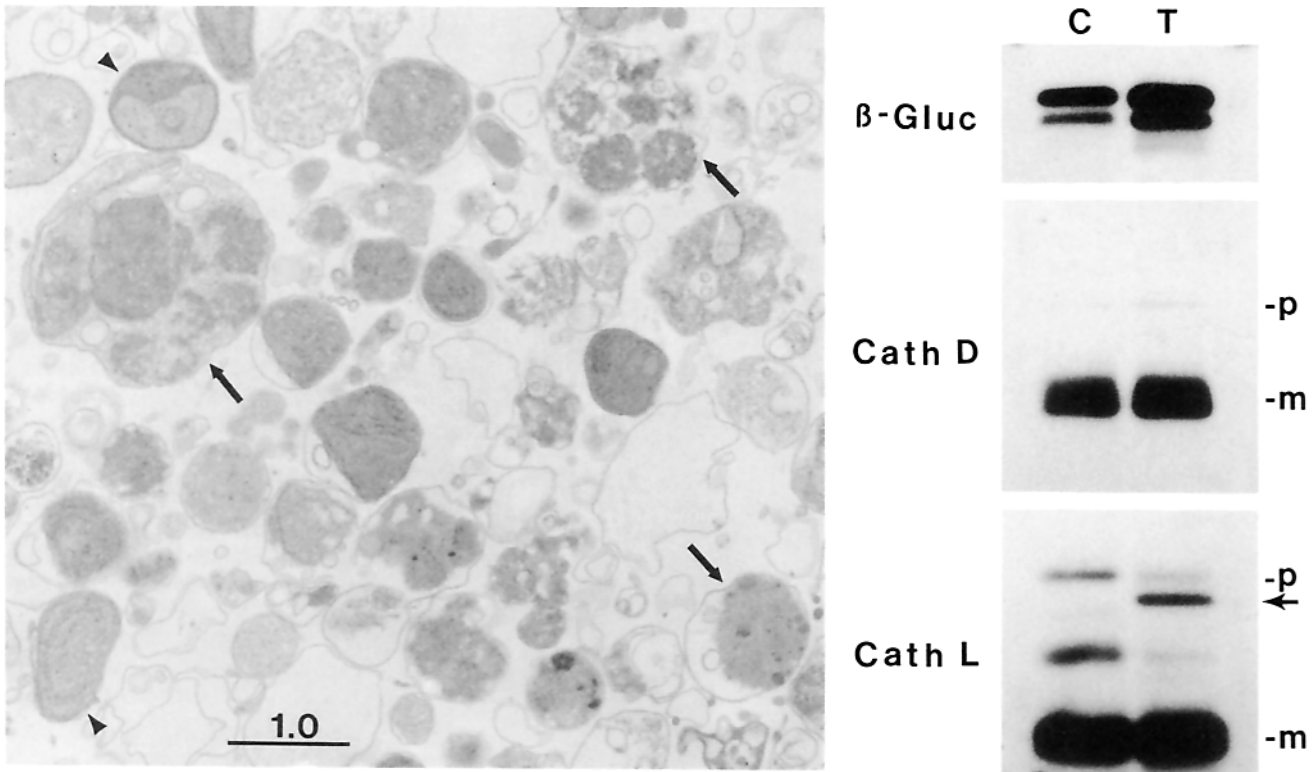


**Figure 8.** Effects of tunicamycin on the amount of lysosomal hydrolases present in autophagic vacuoles isolated from liver homogenates. Rats were fasted for 24 h, the livers excised, and homogenized immediately or perfused with nutrient-depleted media containing tunicamycin (10  $\mu$ g/ml) for 4 h, then homogenized. Fractions enriched for autophagic vacuoles were isolated from the liver homogenates and processed for morphological and biochemical analyses (24). (Left) The preparations consisted of a heterogeneous population of autophagic vacuoles containing recognizable cellular components (arrowheads) and amorphous debris (arrows). Unsequestered mitochondria, peroxisomes, and RER were not visualized. (Right) The presence of  $\beta$ -glucuronidase ( $\beta$ -Gluc), cathepsin D (Cath D), and cathepsin L (Cath L) was determined on Western blots of autophagic vacuole fractions (8  $\mu$ g of protein) obtained from untreated (C) and tunicamycin-treated (T) livers (10, 11). The amount of mature hydrolases present was not altered by tunicamycin treatment. However, in the presence of tunicamycin, an unglycosylated precursor form of cathepsin L was identified (arrow). *p*, precursor form; *m*, mature form. Bar, 1.0  $\mu$ m.

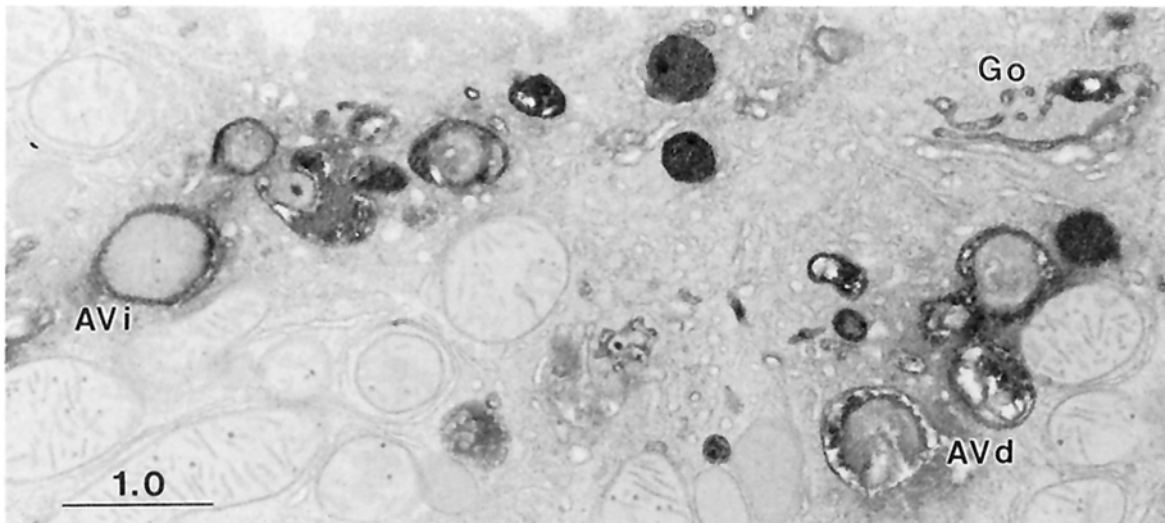


**Figure 9.** Labeling of autophagic vacuoles by *Limax flavus* lectin. Livers were treated as described in Fig. 2, fixed, and tissue sections incubated with *Limax flavus* lectin conjugated to horseradish peroxidase. The peroxidase activity was visualized using methods similar to that described for immunocytochemistry. Labeling was restricted to one or two cisternae of the Golgi complex (Go) and numerous unidentified vesicles. In addition, this lectin labeled both nascent (AVi) and degradative (AVd) autophagic vacuoles. Bar, 1.0  $\mu$ m.

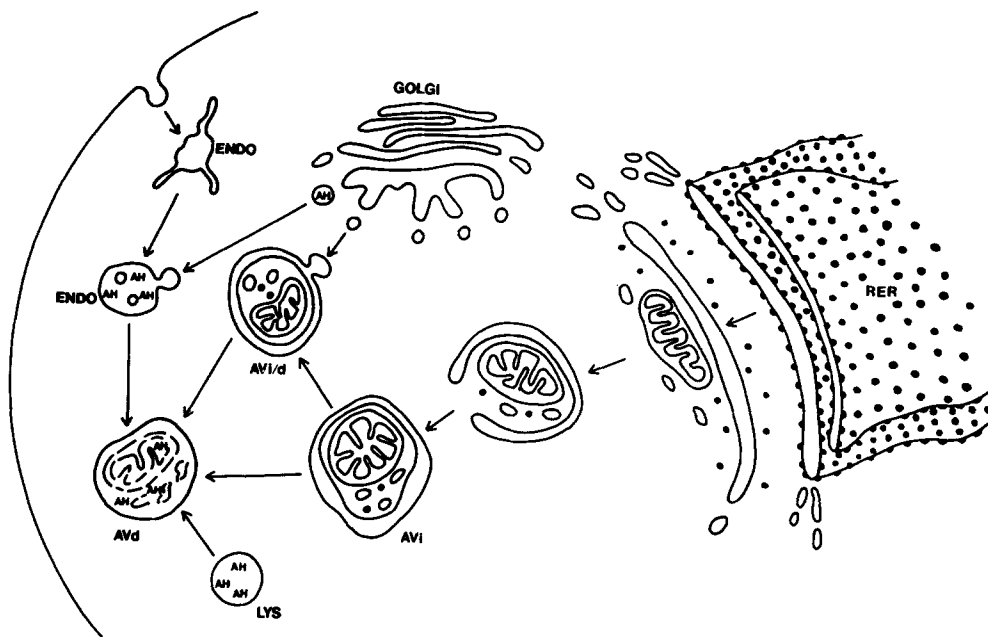


**Figure 10.** Proposed mechanism of autophagy. Upon a stimulus, an invagination of ribosome-depleted rough endoplasmic reticulum (RER) occurs forming a nascent autophagic vacuole (AVi). This vacuole then matures into a degradative vacuole (AVd) by two possible routes: (a) fusion with preexisting lysosomes (LYS) thereby acquiring acid hydrolases (AH) and lysosomal membrane proteins, and (b) acquisition of lysosomal membrane proteins initiating vacuole acidification (AVi/d) before fusion with acid hydrolase containing late endosomes (ENDO) or lysosomes.

terization of the limiting membranes of the three types of autophagic vacuoles will require the isolation of these vacuoles.

The current model of the autophagic vacuole formation and maturation to a degradative lysosome is presented in Fig. 10. My results suggest that maturation of AVis may involve a number of events: (a) incorporation of lysosome membrane proteins; (b) vacuole acidification; and (c) acquisition of lysosome hydrolases. In addition, AVis can acquire both lysosome membrane proteins and hydrolases in a single step by fusing with existing secondary lysosomes. However, the early presence of lysosome membrane proteins could be critical in stabilizing the vacuole membrane and preventing lysis upon delivery of the active hydrolases. Vacuole acidification is not only necessary for active hydrolases but also for IGFII-R/MPR recycling. Acidification of endosomes has been shown to be necessary for recycling of membrane proteins (e.g., IGFII-R/MPR and asialoglycoprotein receptor) (16, 18). The absence of IGFII-R/MPR from AVds present in livers previously treated with leupeptin (unpublished data) suggests protein recycling may be occurring. The occurrence and extent of membrane protein recycling is currently being investigated.

I would like to thank Dr. Ann Hubbard for her helpful discussions and Bill Blakeney for his technical assistance and photographic work. I would also like to thank Drs. Susan Lenk and Brian Hollander for their help in editing the manuscript. Antiserum to cathepsin D was kindly provided by Drs. J. Blum and P. Stahl (Washington University, St. Louis, MO). Antiserum recognizing insulin-like growth factor II receptor (mannose-6-phosphate receptor) was supplied by Dr. S. P. Nissley (National Cancer Institute, Bethesda, MD). *N*-[3-[(2,4-dinitrophenyl)-amino]propyl]-*N*-(3-aminopropyl) methylamine dihydrochloride and mouse anti-dinitrophenol were kindly supplied by Dr. R. G. W. Anderson (University of Texas Health Sciences Center, Dallas, TX). Finally, anti-cathepsin L (major excretory protein) Ig was generously provided by Dr. C. Gabel (Columbia University, New York, NY).

This work was supported by a grant from the National Institutes of Health to W. A. Dunn (AM 33326).

Received for publication 2 November 1989 and in revised form 2 February 1990.

#### References

- Anderson, R. G. W., J. R. Falck, J. L. Goldstein, and M. S. Brown. 1984. Visualization of acidic organelles in intact cells by electron microscopy. *Proc. Natl. Acad. Sci. USA.* 81:4838-4842.
- Arstila, A. U., and B. F. Trump. 1968. Studies on cellular autophagocytosis. The formation of autophagic vacuoles in the liver after glucagon administration. *Am. J. Pathol.* 53:687-733.
- Barriocanal, J. G., J. S. Bonifacino, L. Yuan, and I. V. Sandoval. 1986. Biosynthesis, glycosylation, movement through the Golgi system, and transport to lysosomes by an N-linked carbohydrate-independent mechanism of three lysosomal integral membrane proteins. *J. Biol. Chem.* 261:16755-16763.
- Bartles, J. R., L. T. Braiterman, and A. L. Hubbard. 1985. Endogenous and exogenous domain markers of the rat hepatocyte plasma membrane. *J. Cell Biol.* 100:1126-1138.
- Brown, W. J., and M. G. Farquhar. 1984. The mannose-6-phosphate receptor for lysosomal enzymes is concentrated in cis Golgi cisternae. *Cell.* 36:295-307.
- Brown, W. J., E. Constantinescu, and M. G. Farquhar. 1984. Redistribution of mannose-6-phosphate receptors induced by tunicamycin and chloroquine. *J. Cell Biol.* 99:320-326.
- Chaing, H.-L., S. R. Terlecky, C. P. Plant, and J. F. Dice. 1989. A role for a 70-kilodalton heat shock protein in lysosomal degradation of intracellular proteins. *Science (Wash. DC).* 246:382-385.
- Deter, R. L. 1975. Analog modeling of glucagon-induced autophagy in rat liver. *Exp. Cell Res.* 94:122-126.
- Dunn, W. A. 1990. Studies on the mechanism of autophagy. Formation of the autophagic vacuole. *J. Cell Biol.* 110:1923-1933.
- Dunn, W. A., D. A. Wall, and A. L. Hubbard. 1983. Use of isolated, perfused liver in studies of receptor-mediated endocytosis. *Methods Enzymol.* 98:225-241.
- Dunn, W. A., T. P. Connolly, and A. L. Hubbard. 1986. Receptor-mediated endocytosis of epidermal growth factor by rat hepatocytes: receptor pathway. *J. Cell Biol.* 102:24-36.
- Hasilik, A., and E. F. Neufeld. 1980. Biosynthesis of lysosomal enzymes in fibroblasts. *J. Biol. Chem.* 255:4937-4945.
- Hershko, A. 1988. Ubiquitin-mediated protein degradation. *J. Biol. Chem.* 263:15237-15240.
- Himeno, M., H. Ohhara, Y. Arakawa, and K. Kato. 1975.  $\beta$ -Glucuronidase of rat preputial gland. *J. Biochem.* 77:427-438.

15. Holtzman, E. 1989. Lysosomes. Plenum Publishing Corp., New York. 439 pp.
16. Hubbard, A. L. 1989. Endocytosis. *Curr. Opin. Cell Biol.* 1:675-683.
17. Kiess, W., J. F. Haskell, L. Lee, L. A. Greenstein, B. E. Miller, A. L. Aarons, M. M. Rechler, and S. P. Nissley. 1987. An antibody that blocks insulin-like growth factor (IGF) binding to the type II IGF receptor is neither an agonist nor an inhibitor of IGF-stimulated biologic responses in L6 myoblasts. *J. Biol. Chem.* 262:12745-12751.
18. Kornfeld, S. 1987. Trafficking of lysosomal enzymes. *FASEB (Fed. Am. Soc. Exp. Biol.) J.* 1:462-468.
19. Kreibich, G., B. L. Ulrich, and D. D. Sabatini. 1978. Proteins of rough microsomal membranes related to ribosome binding. I. Identification of ribophorins I and II, membrane proteins characteristic of rough microsomes. *J. Cell Biol.* 77:464-487.
20. Leighton, F., B. Poole, H. Beaufay, P. Baudhin, J. W. Coffey, S. Fowler, and C. deDuve. 1968. The large-scale separation of peroxisomes, mitochondria, and lysosomes from livers of rats injected with triton WR-1339. *J. Cell Biol.* 37:482-513.
21. Lewis, V., S. A. Green, M. March, P. Vihko, A. Helenius, and I. Mellman. 1985. Glycoproteins of the lysosomal membrane. *J. Cell Biol.* 100:1839-1847.
22. Lippincott-Schwartz, J., J. S. Bonifacino, L. C. Yuan, and R. D. Klausner. 1988. Degradation from the endoplasmic reticulum: disposing of newly synthesized proteins. *Cell.* 54:209-220.
23. Louvard, D., H. Reggio, and G. Warren. 1982. Antibodies to the Golgi complex and rough endoplasmic reticulum. *J. Cell Biol.* 92:92-107.
24. Marzella, L., J. Ahlberg, and H. Glaumann. 1982. Isolation of autophagic vacuoles from rat liver: morphological and biochemical characterization. *J. Cell Biol.* 93:144-154.
25. Mellman, I. 1987. Molecular sorting during endocytosis. *Kidney Int.* 32(Suppl. 23):184-195.
26. Mortimore, G. E., A. R. Pösö, and B. R. Lardeux. 1989. Mechanism and regulation of protein degradation in liver. *Diabetes Metab. Rev.* 5:49-70.
27. Nishimura, Y., K. Furuno, and K. Kato. 1988. Biosynthesis and processing of lysosomal cathepsin L in primary cultures of rat hepatocytes. *Arch. Biochem. Biophys.* 263:107-116.
28. Pfeifer, U. 1987. Functional morphology of the lysosomal apparatus. In *Lysosomes: Their Role in Protein Breakdown*. H. Glaumann and F. J. Ballard, editors. Academic Press, Inc., New York. 3-59.
29. Pontremoli, S., and E. Melloni. 1986. Extralysosomal protein degradation. *Annu. Rev. Biochem.* 55:455-481.
30. Reunanen, H., E.-L. Punnonen, and P. Hirsimäki. 1985. Studies on vinblastine-induced autophagocytosis in mouse liver. *Histochemistry.* 83:513-517.
31. Rez, G., and J. Meldolesi. 1980. Freeze-fracture of drug-induced autophagocytosis in the mouse exocrine pancreas. *Lab. Invest.* 43:269-277.
32. Rosenfeld, M. G., G. Kreibich, D. Popov, K. Kato, and D. D. Sabatini. 1982. Biosynthesis of lysosomal hydrolases: their synthesis in bound polysomes and the role of co- and posttranslational processing in determining their subcellular distribution. *J. Cell Biol.* 93:135-143.
33. Rotundo, R. L., K. Thomas, K. Porter-Jordan, R. J. J. Benson, C. Fernandez-Valle, and R. E. Fine. 1989. Intracellular transport, sorting, and turnover of acetylcholinesterase. *J. Biol. Chem.* 264:3146-3152.
34. Sakai, M., N. Araki, and K. Ogawa. 1989. Lysosomal movements during heterophagy and autophagy: with special reference to nematolysosome and wrapping lysosome. *J. Electron Microsc. Tech.* 12:101-131.
35. Schworer, C. M., K. A. Shiffer, and G. E. Mortimore. 1981. Quantitative relationship between autophagy and proteolysis during graded amino acid deprivation in perfused rat liver. *J. Biol. Chem.* 256:7652-7658.
36. Suarez-Quian, C. 1987. The distribution of four lysosomal integral membrane proteins (LIMPs) in rat basophilic leukemia cells. *Tissue & Cell.* 19:495-504.
37. Suarez-Quian, C. 1988. Differential cell surface expression of four lysosomal integral membrane proteins (LIMPs) in normal rat kidney cells. *Tissue & Cell.* 20:35-46.
38. Titus, D. E., and W. M. Becker. 1985. Investigation of the glyoxysome-peroxisome transition in germinating cucumber cotyledons using double-label immunoelectron microscopy. *J. Cell Biol.* 101:1288-1299.